Experimental and numerical study of 3D-printed parts for a pulmonary ventilator circuit

Lara E. P. Santos[1], Daniel F. A. Fontes[1], Julia R. Felipe[1], Mateus A. M. Santos[1], Olexiy Shynkarenko[2]

[1]*Aerospace Engineering Department, Faculty UnB Gama - FGA, University of Brasilia*
Área Especial de Indústria Projeção A, Setor Leste, Gama, 72.444-240, DF, Brazil
lara.emilly@aluno.unb.br, daniel.farkat@aluno.unb.br, juliarfelipe@aluno.unb.br, moura.mateus@aluno.unb.br
[2]*Aerospace Engineering Department - Chemical Propulsion Laboratory, Faculty UnB Gama - FGA, University of Brasilia*
Área Especial de Indústria Projeção A, Setor Leste, Gama, 72.444-240, DF, Brazil
olexiy@aerospace.unb.br

Abstract. The speed of propagating COVID-19 has culminated in an alert from the World Health Organization, characterized by a global health problem and an emergency state. In Brazil, the growing demand for obtaining spare parts for respirators motivated researchers of the University of Brasilia to assist in the task force of providing studies in this area. The 3D printing could be a solution for the low-cost respirator parts replacement attending ISO standards. Such verification is the main objective of the current work. The structural integrity tests showed the agreement of the 3D-printed parts with the ISO 80601-2-80 technical requirements. The numerical simulations were based on the transient Navier-Stokes equations to study the flow patterns in a ventilator circuit with original and printed components. The geometry discretization method took into account boundary layer and flow recirculation zones. The following studies have been analyzed: simulation of the flow path built from the original components and 3D-printed components, doubled flow circuit for two patients, and an evaluation of the usability of the newly fabricated parts. The simulation results showed reduced pressure losses and improved flow patterns for the newly designed 3D-printed parts and their complete attendance to the ISO requirements to medical connections.

Keywords: Pulmonary ventilator, Numerical simulation, COVID-19, Transient flow, Breathing cycle

1 Introduction

At the end of 2019, the world was affected by the new Coronavirus. Since then, according to Dasa [1], all countries have mobilized to contain the spread of this disease as thousands of new cases appear daily. More severe cases of this infection present difficulty for breathing and, when the ability to breathe on their own is lacking, the patient must be intubated. During intubation, the pulmonary ventilator assists the person. This device partially or fully favors the breathing process by sending a gas mixture to the patient during inspiration, waiting for gas exchange time. The Brazilian Ministry of Health [2] states that the ventilator can program accounts for some parameters, such as gas pressure or volume, and then allows the liberation of gases from expiration.

There is a high worldwide demand for pulmonary respirators and spare parts due to the pandemic caused by the Sars-CoV-2 virus. The researchers at the University of Brasília have been looking to facilitate the authorities' access to the necessary equipment.

Current work aims to evaluate the possibility of implementing 3D-printed connections as a low-cost solution for respirator parts replacement by mechanical testing and numerical simulation of the flows. The research is based on existing ABNT [3] norms that regulate the use and manufacture of connectors used for medical purposes.

Also, the current work aims to verify the possibility of using a double ventilatory circuit of a Puritan Bennett 800 Series Ventilator System used as reference. It should utilize parts manufactured by 3D printing and would feed the respiratory system of two patients. The numerical study will analyze the total capacity of the used ventilator, determining the efficiency and then the applicability of this circuit.

To study the efficiency and applicability of printed connectors to the original ones already used in market analyzes and numerical study will be used with the aid of commercial simulation software for the estimation of the flow parameters based on the work of Anderson [4] and Enayer, Gibson, Taylor and Yianneskis [5].

In search of precise and adequate results to the location where this study was conducted, it was necessary to find a model patient. According to the Brazilian Intensive Care Medicine Association (AMIB) [6], men at the age of 61 were the majority at Intensise Care Units (ICU) at the time of the research and IBGE [7] points out an average height of 1.68 m and weight of 73 kg for people on that age in Brazil. The Authors use such requisites as initial parameters for the current research. The Didactic Mechanical Ventilato Simulator (SDVM) [8] has been used for the boundary conditions calculation in the numerical study.

The complete analysis and comparison of 3D printed parts to the original ones will allow deciding the applicability of the additive manufacturing technology in the substitution of pulmonary ventilator spare parts.

2 Methodology

2.1 Experimental study

ABNT ISO 5356 standard [3] presents requirements for 22 mm lock cones and sockets, including performance requirements. There are four types of tests to be performed according to the standard: coupling with cones, leak test, drop test, measurement of diameters. Figure 1 shows the benchtop apparatus for performing safety testing of a 22 mm locking socket coupling according to ISO 5356-1:2016. Here, 1 is the support, adjustable for torque application, 2 is the adapter, 3 is the Y1 adapter, 4 is the 22 mm test part (Y - original), 5 is the 22 mm test part (Y - modified), 6 is the Y2 adapter, 7 is the axial load gauge: BTS S20, 8 is the Y3 adapter, 9 is the adjustable axial force adapter 10 is the torque meter.

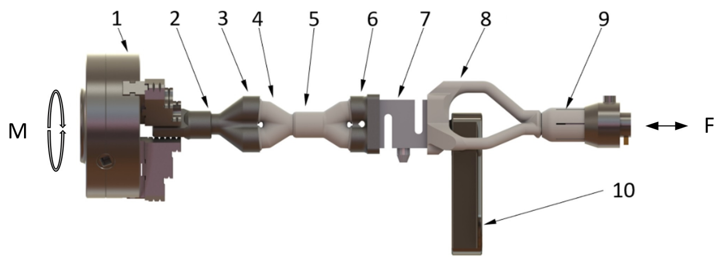

Figure 1. Apparatus for coupling of locking sockets safety testing

The measuring instruments are thermocouple of K-type Omega CLAD, load cell Full Bridge BTS S20 - 20 kg, mechanical torque wrench TRNA20PA, data acquisition system National Instruments cDAQ 9178, module 9237. Measurement errors: forces and moments - up to 2%, temperatures - up to 1 C. Number of samples: original Y type (Yo) - 5 units, modified Y type (Ym) - 5 units, type I - 5 units.

Measurement errors are for forces and moments - up to 2%, temperatures - up to 1°C. Number of samples: original Y type (Yo) - 5 units, modified Y type (Ym) - 5 units, type I - 5 units.

2.2 Numerical study

Figure 2 represents the computational domains of Y-connectors for the flow simulations for both original parts (a) and modified one (b) manufactured with 3D printing. Here, edge (1) represents the flow inlet in the inspiration part of the breathing cycle, edge (2) is the outlet in the expiration regime, and edge (3) is the outlet in the inspiration regime and inlet in the expiration regime. The connections (1) and (2) are also assembled to the standard flexible piping of 15.4 mm diameter and one-meter length. These pipes are also part of the computational domain. However, they will not be demonstrated due to excessive lengths.

Figure 2 shows that there are two geometrical symmetry planes in both computational domains. One lies in the middle vertical plane, and the other is in the horizontal plane. Such a factor potentially reduces four times the computational time. But, analyzing the respiration cycle (Fig. 2c) as boundary conditions, the authors found that only a vertical plane can serve as symmetry due to the presence of two flow phases (inspiration and expiration).

The boundary conditions used in the numerical simulation were obtained from Didatical Mechanical Ventilator Simulator [8] using as input data the necessary flow parameters for a 61 years old male patient, height $H = 168$ cm and weighing 73 kg, setting the system as "volume control." According to AMIB and the Brazilian Society of Pulmonology and Phthisiology (SBPT) [9], it is recommended to use 6 ml/kg initially predicted in the volume,

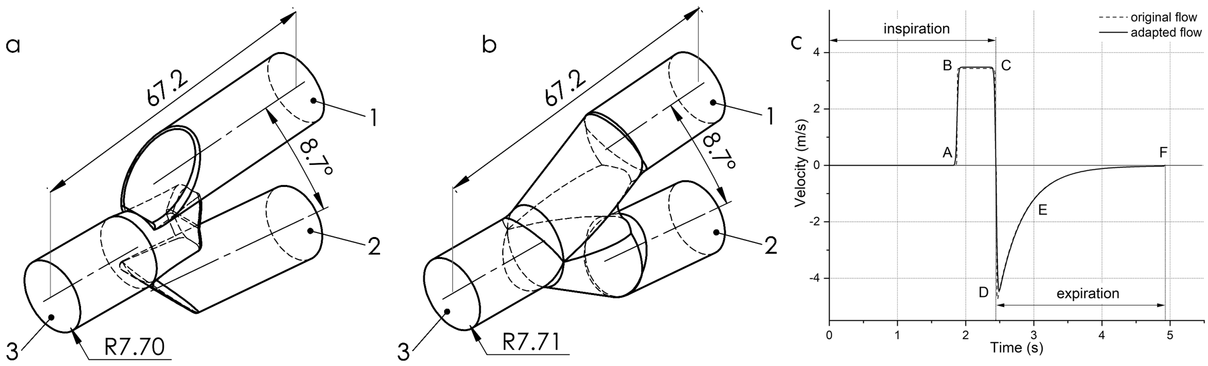

Figure 2. Computational volumes of original (a) and modified (b) components and inlet flow velocity (c)

with the expected weight being calculated below, the respiratory rate from 12 to 16 bpm (breaths per minute), inspiratory pause from 0.3 s to 0.5 s and airflow between 40 and 60 L/min. Then, the data used in the simulator for the given patient were 390 ml of volume, 12 bpm, 0.5s inspiratory pause, and 40 L/min flow, with the other parameters left at their default values.

$$P = 50 + [0.91(H) - 152.4] \tag{1}$$

Thus, the authors obtained the flow graph in the simulator, and, in this way, it was possible to get the values at various points to prepare a file with these data. However, the boundary condition used in the numerical simulation was the flow velocity, found through the mass flow formula below substituting the flow values, the connector inlet area, and the air density (considered 1.2754 kg/m^3).

$$\dot{m} = \rho A V \tag{2}$$

The velocity gradient should be compatible with the method of solution and the Courant number. Fig. 2c shows the ”adapted” inlet velocity for the numerical simulation. The figure represents the change of velocity for a respiratory cycle of 4.93 s long. It is possible to observe inspiration and expiration phases. The point “A” represents the beginning of the inspiratory phase. “B” is the active phase of inspiration which finishes at point “C.” On the curve “D-E-F,” the expiration phase occurs. After, the respiration process repeats.

The authors constructed the mesh on one-half of the connector due to its transversal symmetry. It is more detailed in the central part of the connector. The long ends of the cylindrical tube have elongated cell refinement because they are simulated to provide realistic flow behavior to the Y-connectors.

The mesh confection consists of two parts: the cylindrical tube and connector. The face meshing tool was applied to all the faces of the computational domain. The cylindrical tubes were divided using the edge sizing function with the corresponding Bias factor to build the boundary cells layer structure in radial and axial directions and refine it near the connector. The connector was discretized using the inflation function, automatically creating the boundary layer mesh and refining the computational volume. In the end, the mesh of the original geometry (Figure 3) has 232,840 elements, and the mesh of the proposed geometry (Figure 4) has 388,219 cells.

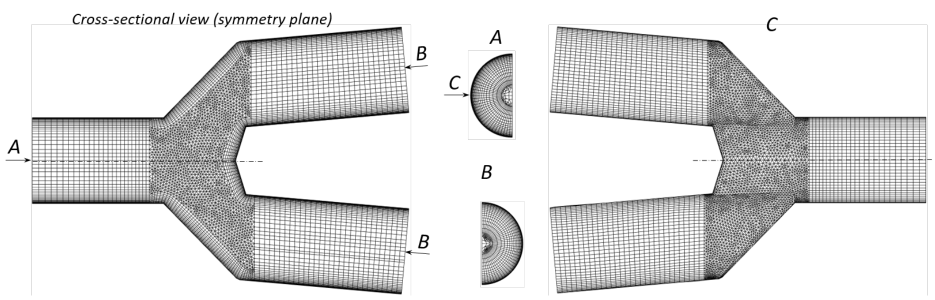

Figure 3. Meshing of the original geometry

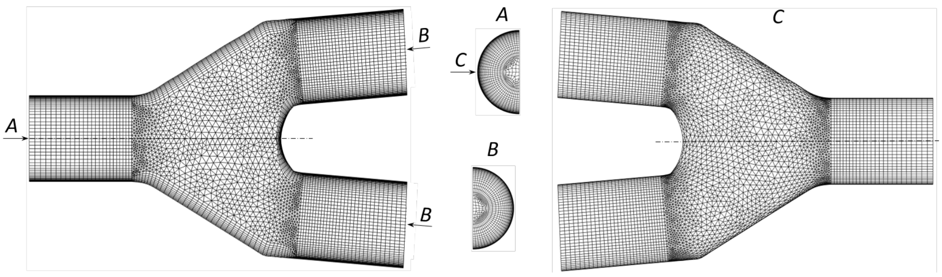

Figure 4. Meshing of the proposed geometry

In the images above, it is possible to observe the discretization result of both geometries. The boundary layer of cells along its wall and the structured mesh in the cylindrical tube are noticeable, as seen in details A and B of Fig. 3 and 4.

The authors performed the analysis of steady flow using a constant velocity inlet of 3 m/s to validate the mesh and analyze the behavior of the boundary layer. The research was performed on the Y-connector with the one-meter long tubes connected to both of the connector openings, positioned to represent the tubes connected to the mechanical ventilator. Ten radially-directed control lines (probes) were defined in the cylindrical pipe with a spacing of 100 mm to study the propagation of the boundary layer.

According to Enayer et al. [5], Takamasa and Tomiyama [10], the velocity profiles are normalized by the inlet velocity. The space coordinate was dimensioned by the tube radius, where a dash denotes the normalized variables. The velocity gradient is normalized by its maximum experimental value.

$$\bar{y} = \frac{y}{r},\ \bar{u} = \frac{u}{V_\infty},\ \nabla\bar{u} = \frac{du}{dy}/max(\frac{du}{dy}) \tag{3}$$

The simulation model bases on the averaged Navier-Stokes equations coupled with the k-omega SST model of turbulence. The equation system solved in Ansys Fluent utilizes the third-order method of approximation in spatial directions, the second-order method of turbulent parameters discretization, and the first-order implicit method by time.

From the boundary conditions obtained through the SDVM [8], simulations of viscous flows were carried out for the original and modified connectors. The simulation consisted of 2 steps representing the respiratory cycle. In the first of them, the inspiration stage, the flow inlet was a boundary of one-meter cylindrical tubes (1), Fig. 2, connected to the medical device. The outlet was the boundary (3) of the connector socket connected to the patient. In the second stage (the expiration phase), the flow enters from (3) and exits to the second pipe (2).

To prove that the modified part produced by additive manufacturing has better flow characteristics than the original part, the authors provided a study about the efficiency of both elements. This analysis calculates the total pressure drop in both original and modified connectors during the entire breathing cycle. According to Anderson [11], the total pressure quantitatively indicates the capacity of a flow to do useful work. Thus, the flow loses some of this potential when there is a loss of the total (stagnation) pressure. Herbert in [12] further states that, in general, the losses of stagnation pressure in a pipe or channel are due to friction, with the contribution of gravity and acceleration.

The total pressure difference identifies the part with a minor stagnation pressure difference on a global scale. It, by consequence, indicates a more efficient flow. The area-weighted average total pressure was taken at the edges of each connector in every instant of time. The time integral of the stagnation pressure difference defines the total losses on Y-connector during the respiration cycle.

3 Results

3.1 Double flow analysis

In the pandemic caused by the COVID-19 many deaths could be avoided if there was a way to optimize the equipment used. The following numbers show that there is a possibility of using the same mechanical ventilator on two patients simultaneously, which would minimize the cost and difficulty of maintenance of the respirators, which are essential for the treatment of severe cases. The “Puritan Bennett™ 800” respirator technical reference manual [13], the one used in this study, has the maximum flow of oxygen pump of 200 L/min, aiming to control the SpO2. It reveals how much oxygen the body’s organs are receiving. But, in the severest cases of the disease, according to

AMIB and SBPT [9], the maximum use required per person is 40 L/min. In other words, any respirator can pump in oxygen around five times more than a human being, in its worst breathing conditions, needs.

Without going any further, it is necessary to emphasize that treatment protocols must be followed to achieve this use of respirators, and extra attention must be taken to associated risks. The protocol, according to Beitler, Kallet, Kacmarek et al. [14], is used to intubate two patients victims of COVID-19. The patients must be in similar respiratory clinical conditions. It informs that, if the protocols are not followed, among the problems of using the same respirator, one is the increase in cases of accidental extubation for each respirator, which would result in the system being disconnected. Something important to be remembered is that after an extended period, one respirator will be needed for each patient, what doesn't minimize at all the significant effect of optimized use of respirators in a pandemic scenery, even if it's only during some time of the treatment.

From an aerodynamic point of view, according to AMIB and SBPT [9] and the ventilator technical reference manual [13], it is possible to use a respirator for two patients with similar comorbidities using the maintenance and preparation procedures studied by Beitler et al. [14]. Increasing the oxygen flow by adding 3D printed parts, future studies exploring that could optimize ventilator use when the respirator is used in two patients.

3.2 Experimental results

According to the standard, the test samples were placed in the oven in the humid environment for 60 minutes. The samples were marked as shown in Fig. 5a. Two groups of Y-type parts received the names from Ym-1 to Ym-5 and from Yo-1 to Yo-5, respectively. Test coupling of I-type received names from I-1 to I-5. After the humid conditioning, the samples were assembled in couplings to create any possible combinations of parts Ym and Yo, a total of 25. The parts couplings have been installed on the test stand according to Fig. 1, and connected to the moment and force measure equipment (Fig. 5c).

Tests executed according to the ABNT Standard [3] showed correspondence of the forces and moments to the decoupling requirements of the conical surfaces for medical applications. Figure 5 shows the test on decoupling force application with a momentum of 30 N·cm. The slight compression force of 10 N was applied during the first 5 s of the test. After, the expansion force was applied during 35 s. The measurement error is near 1.5%.

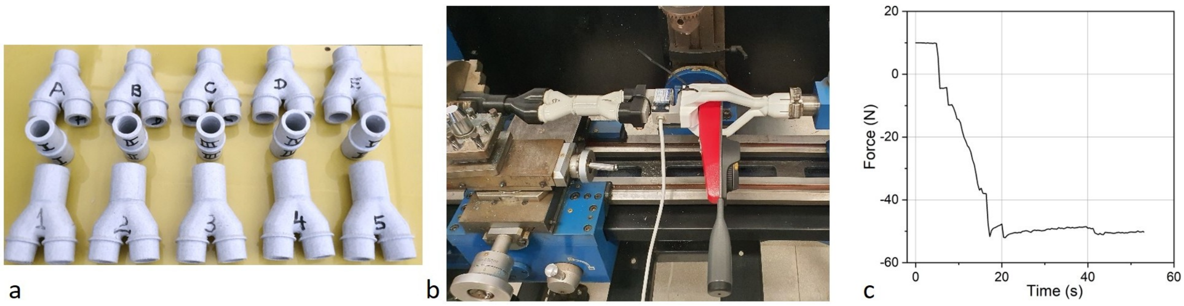

Figure 5. The test execution: parts marking (a), test setup (b), and experimental results (c)

The leakage tests applied to all the 15 parts (Ym, Yo, and I-type) showed the following. The sample Ym-3 presented a maximum leakage of 3.65 ml/min. Six samples did not show any leakage during the five-minute testing. The rest eight samples showed minor leakage; the average flow among all the tests was 0.952 ml/min. The drop test was successful for all fifteen samples ensuring their excellent mechanical resistance. The connection size measurement test showed the following. According to the standard, the coupling size should be 22.425 $\pm$ 0.005 mm. The average measured connection diameter is 22.533, and the standard deviation is 0.0726 mm.

Analyzing the size measurement results, one may find their not strict correspondence to the ISO Standard. Nevertheless, such an analysis should consider the following two factors. First, the plastic material of samples is flexible, so the shape changes are possible with slight force application. Second, the reference samples acquired from certified suppliers presented much more significant size divergence and deviations than 3D-printed samples.

3.3 Numerical results

Figure 6a shows distributions of the dimensionless velocities and velocity gradients along the straight one-meter cylindrical pipe. According to these results, the turbulent boundary layer occupies near 20% of the flow area.

The results obtained are satisfactory, considering that there is no slipping in the regions too close to the boundary layer. Due to this condition, according to Anderson [11], near the tube wall, the velocity is close to zero and having a more significant velocity gradient. In Fig. 6a, the tube wall corresponds to $y = 0$, and the tube center is at $y = 1$. From that, it is possible to observe all of the conditions presented previously. Besides that, the velocity distributions are similar to those found in experimental data provided by Enayer et al. [5] and Takamasa et al. [10], reinforcing the validity of the results.

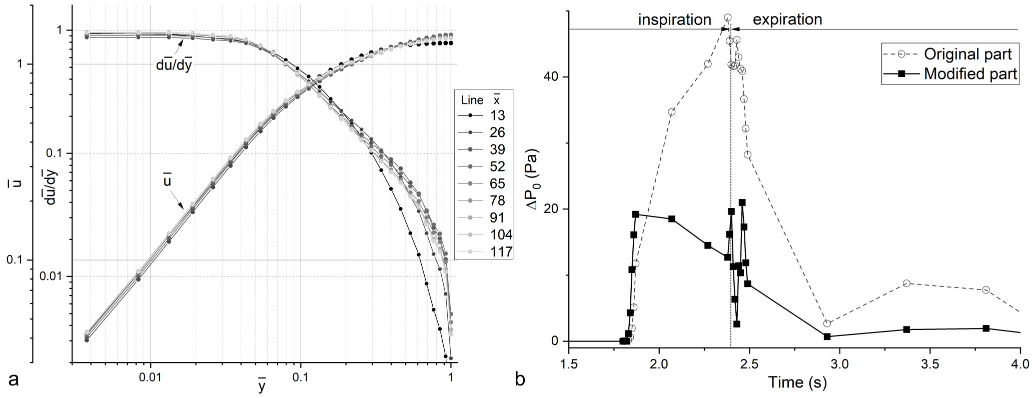

Figure 6. Simulation results: velocity and its gradient along the cylindrical pipe (a) and total pressure drop (b)

Fig. 6b shows that the modified part presented more minor stagnation pressure losses in both the inspiration and expiration phases to the original component. The integral of the stagnation pressure losses in time for the original part is 37.5 Pa·s, and the modified one is 14.6 Pa·s. So, it is possible to observe that the modified part had a better performance, presenting a total pressure loss of 61% less than the original part.

Figures 7 and 8 show the pathlines in the original and modified connector in the inspiration and expiration phases, respectively. These results indicate that its geometry constrains the flow in the original connector due to the rapid change of the flow direction and crossectional area. It creates high-magnitude velocity up to 10 m/s in the transition region and intensive turbulence, resulting in high energy losses. On the other hand, the modified geometry simulation has smooth area behavior in the flow path. The flow velocity in the transition region is smaller (7.5 m/s) than in the original part, and the intensive flow separation in the inspiration regime is not observed. As a result, the pressure losses are significantly lower.

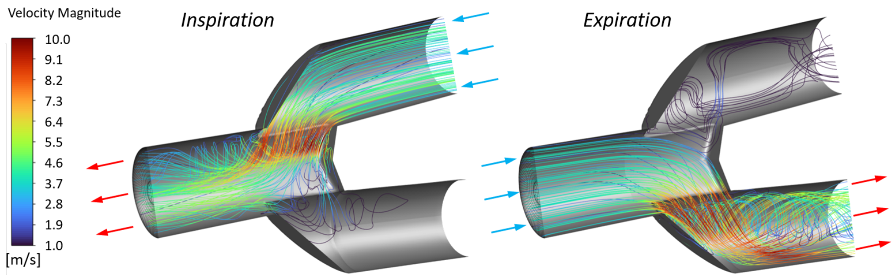

Figure 7. Flow in the original geometry

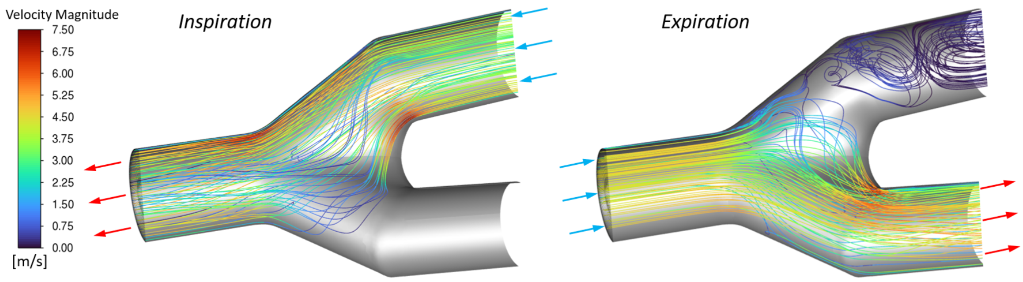

Figure 8. Flow in the proposed geometry

The original part has a higher number of vortices for the expiration process and a lower velocity flow at the end. The modified part has a faster and smoother flow. From that information, the authors conclude that the modified component is more efficient on flow transportation in both phases of the respiration cycle.

4 Conclusions

The mechanical tests showed that all connections supported forces and unlocking moments for a determined time, according to the standard ABNT ISO 5356-1. Leakage is within the norms. There is no evidence of damage to parts after drop testing. The geometrical sizes have acceptable tolerances to ensure a reliable operation of 3D printed parts.

Regarding the boundary layer analysis, with the aid of Fluent simulation, it was possible to observe its presence and influence when analyzing the no-slip condition on the tube wall and the curves obtained, thus validating the computational mesh.

In terms of the efficiency analysis, it is possible to conclude that, in general, the parts which are made with additive manufacturing are more efficient than those which are produced to date. From the flow perspective, even though they have more significant values of total pressure difference in the expiration phase of the breathing cycle, the modified part presented a loss of full pressure 61% smaller than the original part.

From the aerodynamic point of view, using a 3D printed part in the sharing mechanical ventilator speeds up the recovery of Covid-19 patients. On the other hand, it is also essential that the clinical and mechanical compatibility tests have been completed successfully.

Acknowledgements. The authors would like to acknowledge the University of Brasilia and the Chemical Propulsion Laboratory of UnB for the financial and technical support of the research project.

Autorship statement. The authors hereby confirm that they are the sole liable persons responsible for the authorship of this work, and that all material that has been herein included as part of the present paper is either the property (and authorship) of the authors, or has the permission of the owners to be included here.

References

[1] Dasa. COVID-19: all about coronavirus, symptoms and how to prevent, 2021.
[2] BRAZIL Ministry of Health. Brazilian Guidelines for Hospital Treatment of Patients with COVID-19, 2021.
[3] ABNT (Brazilian Association of Technical Standards). ABNT NBR ISO 5356-1 Anesthetic and respiratory equipment - Cone connectors. Part 1: cones and sockets, 2016.
[4] D. Anderson, J. C. Tannehill, and R. H. Pletcher. *Computational Fluid Mechanics and Heat Transfer*. CRC Press, 3ª edition, 2016.
[5] M. Enayer, M. Gibson, A. Taylor, and M. Yianneskis. Laser Doppler Measurements of Laminar and Turbulent Flow in a Pipe Bend. *Znt. J. Heat & Fluid Flow,*, vol. 3, pp. 213–219, 1982.
[6] BRAZIL AMIB (Brazilian Intensive Care Medicine Association). Brasilian ICUs, 2021.
[7] IBGE (Geography and Statistics Brazilian Institute). Research on family budgets - table 2645, 2008.
[8] BRAZIL UFSC (Federal University of Santa Catarina). Mechanical Ventilation Didatic Simulator, 2016.
[9] AMIB (Brazilian Intensive Care Medicine Association) and SBPT (Brazilian Society of Pulmonology and Phthisiology). Brazilian Guidelines on Mechanical Ventilation, 2013.
[10] T. Takamasa and A. Tomiyama. Three-Dimensional Gas-Liquid Two-Phase Bubbly Flow in a C-Shaped Tub. In *International Topical Meeting on Nuclear Reactor Termal Hydraulics*, volume 9, 1999.
[11] J. Anderson. *Fundamentals of Aerodynamics*. McGraw-Hill Science/Engineering/Math, New York, 5th revised ed. edição edition, 2010.
[12] K. Mayes and H. Oertel jr. *Prandtl's essentials of fluid mechanics*, volume 158. Springer Science & Business Media, 2004.
[13] Nellcor Puritan Bennett LLC. The Puritan Bennett™ 840 Ventilator System: Operator's and Technical Reference Manual, 2010.
[14] J.R. Beitler, R. Kallet, R. Kacmarek, and et al. Ventilator Sharing Protocol: Dual-Patient Ventilation with a Single Mechanical Ventilator for Use during Critical Ventilator Shortages, 2020.